Journal of Molecular Modeling (2021) 27: 7
https://doi.org/10.1007/s00894-020-04656-2

ORIGINAL PAPER

Pressure effects on electronic, elastic, and vibration properties of metallic antiperovskite $PbNCa_3$ by ab initio calculations

Yasemin O. Ciftci [1] · Meryem Evecen [2] · İrem O. Alp [1]

Received: 6 April 2020 / Accepted: 21 December 2020 / Published online: 3 January 2021
© The Author(s), under exclusive licence to Springer-Verlag GmbH, DE part of Springer Nature 2021

Abstract

Ab initio computations are performed to study the structural, elastic, electronic, and vibrational characteristics of the cubic antiperovskite compound $PbNCa_3$ under pressure up to 50 GPa. By using the generalized gradient approximation (GGA), the equilibrium structural parameters, energy band structure, density of states, elastic properties, and phonon frequencies for $PbNCa_3$ have been examined. We have obtained some concerned feature as Young modulus and Poisson ratio for this compound using the elastic parameters. The computed elastic constant values show that $PbNCa_3$ is stable up to 30 GPa as mechanically. To assess the stability of this compound dynamically, we have investigated the one-phonon DOS and phonon dispersion relations under pressure. Our results indicate that the calculated structural parameter values at 0 GPa are in accord with the existing data.

Keywords Antiperovskite · Elastic properties · Electronic structure · Phonon · Ab initio calculations

Introduction

Perovskite materials have a formula of ABX_3, where A and B are cations and X is an anion [1, 2], while in the case of antiperovskite, the positions of cations and anions interchange. The crystal structures of both types of materials are similar and can be used in the fields such as semiconductors, fuel cells, batteries, sensors, membrane reactors, and hydrogen production. Antiperovskite materials can extract waste heat and turn it into electricity, making them interesting for any industrial application [3]. Cubic antiperovskite compounds, including carbides and nitrides, have different technological applications due to physical properties such as giant magnetoresistance [4], nearly zero temperature coefficients of resistivity [5], and wide range of band gaps, from super conductor to insulator [6, 7]. The general formula for these compounds is AXB_3, where A is group III–V element, X is carbon or nitrogen, and B is s–d metal [8, 9]. These materials crystallize in a cubic structure with space group Pm3m (#221). These properties make these compounds useful for applications such as to read data from hard disk drives, biosensors, microelectromechanical systems (MEMS), and other devices. Moreover, these compounds exhibit excellent mechanical properties [10–12] which make their possible utility in automobiles and space technology.

Antiperovskite materials have been studied mostly from many researchers. Experimentally, $XNCa_3$ was synthesized by mixing and powder pressing of Ca_3N_2. Then the X (X = Ge, Sn, and Pb) element was put into a pellet, and later, the pellet was heated at 1000 °C in flowing dry N_2 gases [13]. From the theoretical side, Chern et al. [13] have studied the phase transition of $MNCa_3$ (M = P, As, Sb, Bi, Ge, Sn, Bi) and seen that there are phase transitions from cubic to orthorhombic for $PNCa_3$ and $AsNCa_3$. It is found that $SbNCa_3$ and $BiNCa_3$ cubic antiperovskite compounds are semiconductors by Moakafi et al. [14]. For different volumes, total energy are calculated to obtain the ground state properties, and the calculated total energy-volume data are fitted to Murnaghan's equation of state (EOS) to obtain lattice parameters, bulk modulus, and its first order pressure derivatives [15]. $TiNCa_3$ and $AuNCa_3$ have been found to be metallic [16, 17]. The bonding properties and electronic structure of $BiNCa_3$ and $PbNCa_3$ using ab initio method have been investigated by Papaconstantopoulos et al. [18]. Later, Vansat et al. [19] have performed the structural properties of $AsNCa_3$, $PNCa_3$, and $BiNCa_3$ using local density approximation (LDA) and are also of the opinion that $BiNCa_3$ is a narrow band gap semiconductor. The structural, electronic, and elastic

✉ Yasemin O. Ciftci
yasemin@gazi.edu.tr

[1] Physics Department, Faculty of Arts and Sciences, Amasya University, 05100 Amasya, Turkey

[2] Department of Physics, Gazi University, Teknikokullar, 06500 Ankara, Turkey

properties of the cubic antiperovskite $XNCa_3$ (X = Ge, Sn, Pb) have been calculated using density functional theory (DFT) within pseudo-potential plane wave method (PP-PW) by Haddadi et al. [2]. Haddadi et al. [20] have investigated structural and elastic properties of $ANCa_3$ (A = P, As, Sb, and Bi) under pressure. They [2, 20] have calculated bulk modulus and its pressure derivatives of $XNCa_3$ by fitting pressure-volume data to third-order Birch-Murnaghan equation of state (EOS) [21]. The electronic and optical properties of $GeNCa_3$ were studied by Igbal et al. [22]. Also, Iyigor et al. [23] have studied the mechanical, electronic, vibrational and thermodynamical properties by means of generalized gradient approximation approach within the DFT. Here, to obtain lattice constants and bulk modulus, total energies were matched to Murnaghan EOS [15]. Lately, Bilal et al. [24] have studied metallic thermoelectric materials. The authors have investigated the thermoelectric properties of metallic antiperovskites $ANCa_3$ (A = Ge, Sn, Pb), $BCFe_3$ (B = Al, Zn, Ga), and $SnCD_3$ (D = Co and Fe) based nitrogen and carbon using the first principles calculations [24].

Despite these given results, some of the physical properties of $PbNCa_3$ compound are yet scarce in the available literature. Also, there are no calculations exploring the vibrational properties of this perovskite structure and pressure effect. A detailed study of the same properties of $PbNCa_3$ is needed to realize its potential applications in technology. This has motivated us a theoretical analysis of the structural, elastic, electronic, and vibrational properties of $PbNCa_3$ under pressure.

The paper is organized as follows: in the following section, we give computational methods. The important results of our findings are separately presented in section Results and discussion for each property of that system, followed by a conclusion.

Methods

In this work, the first principles calculations have been performed using Cambridge Sequential Total Energy Package (CASTEP) simulation software [25], based on density functional theory [26]. By means of the self-consistent field (SCF) iteration, a density-mixing minimization method, the electronic wave functions are firstly obtained. Then optimized structure has been obtained by using the method of Broyden, Fletcher, Goldfarb, and Shannon (BGFS) [27] under various hydrostatic pressures ranging from 0 to 50 GPa. Perdew-Burke-Ernzerhof (PBE) [28] using Vanderbilt Ultrasoft pseudopotential was enforced for the exchange-correlation terms. Generalized gradient approximation (GGA) was also considered for the electron-electron interaction. The kinetic energy cutoff is taken to be 600 eV for the wave function. The crystal reciprocal-lattice and integration over the Brillouin zone is applied using a 12 × 12 × 12 Monkhorst-Pack [29] k-points sampling procedure for antiperovskite $PbNCa_3$ to geometry optimizations and energy calculations. Pb $5d^{10}6s^26p^2$, N $2s^22p^3$, and Ca $3s^2\ 3p^64s^2$ electrons are taken as valence electrons. The maximal Hellmann-Feynman force converge criterion between atoms, the maximum ionic displacement, and the maximum stress are 0.001 eV/Å, 5.0×10^{-5} Å, and 0.002 GPa, respectively.

Results and discussion

Structural properties

The ternary calcium nitrides $PbNCa_3$ having Pb from the group IV pertain to the nitrides of antiperoveskite-type. The structure of ideal cubic antiperovskite for $PbNCa_3$ materials (#221) includes one formula with the Wyckoff positions of the atoms which are Pb 1a (0, 0, 0), N 1b (0.5, 0.5, 0.5), and Ca 3c (0, 0.5, 0.5) as seen in Fig. 1 . For the calculation of the ground state features of the $PbNCa_3$ compound, the total energy is computed at different volume ranges from 1.5 V_0 to 0.5 V_0, where V_0 is the equilibrium volume of unit cell. The computed total energy-volume data are fitted to the Murnaghan's EOS [15] and a third-order Birch-Murnaghan EOS [21] for the determination of the ground state features including the bulk modulus B_0, its pressure derivatives B_0', equilibrium lattice parameter a_0, volume (V_o), and total energy at $P = 0$ GPa and T = 0 K. The obtained results of the PbNCa3 and similar $XNCa_3$ (X = Ge, Sn, Bi, Sb, P, As) compounds and their comparison with the other theoretical and experimental values can be seen in Table 1. It is shown in the Table 1 that the computed values of the lattice constant (a = 4.942 Å) are in good agreement with the experimental data (a = 4.955 Å) [13] and slightly higher than the theoretical value (4.9197 Å) [2]. In this study, for both EOS, better agreement is obtained with experimental result within 0.26% for PbNCa3 than another theory [2]. This provides the reliability of the present first principles calculations. Comparing lattice parameter for $PbNCa_3$

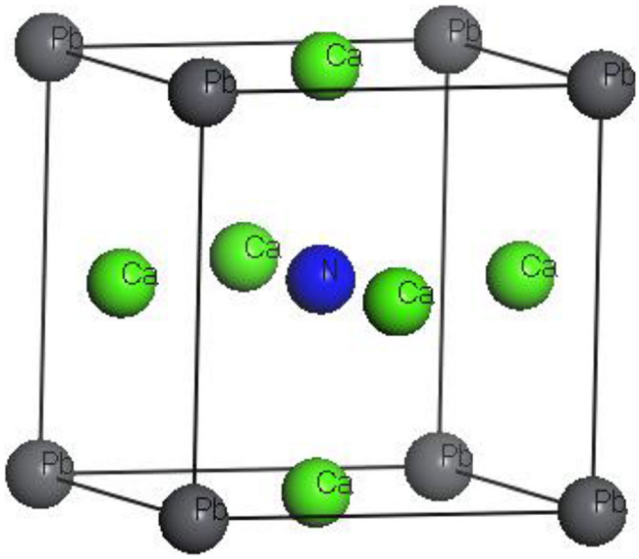

Fig. 1 The unit cell of the $PbNCa_3$

Table 1 Computed lattice parameters a_0, bulk modulus B_0, pressure derivatives of bulk modulus B_0', equilibrium volume V_0, total energy E_{tot} (eV), and other results for $XNCa_3$

Reference	a_0 (Å)	B_0 (GPa)	B_0'	V_0 (Å^3)	E_{tot} (eV)
Present(Mrn_1)	4.942	49.61	4.25	121.26	− 4938.84
Present(BrMrn_2	4.942	49.67	4.23	121.26	− 4938.84
Theor.	4.9197[a]	51	4.2		
Exp.	4.955[b]				
$GeNCa_3$	4.78[a]	58[a]	3.99[a]		
	4.807[d]	56.324[d]			
$SnNCa_3$	4.86[a]	56[a]	4.02[a]		
$BiNCa_3$	4.916[c]	54.18[c]			
	4.918[e]	54.01[e]	4.5[e]		
	4.864[f]	57.07[f]	4.02[f]		
$SbNCa_3$	4.87[c]	57.64[c]			
	4.862[e]	55.42[e]	4.95[e]		
	4.891[f]	60.90[f]	3.97[f]		
$PNCa_3$	4.703[f]	65.95[f]	3.95[f]		
$AsNCa^3$	4.757[f]	60.50[f]	4.17[f]		

[a] Ref [2], [b] Ref [13], [c] Ref [30], [d] Ref [23], [e] Ref [14], [f] Ref [20]

Mrn_1: Murnaghan EOS

BrMrn_2: Birch Murnaghan EOS

with those of other similar compounds ($XNCa_3$), the lattice constants of $PbNCa_3$ is the biggest one among the others, which is due to the fact that the radius of the Pb (1.80 Å) is the biggest one among Ge (1.25 Å), Sn (1.45 Å) from group VI, and P (1.0 Å), As (1.15 Å), Sb (1.45 Å), and B (1.60 Å) from group VII. It also can be seen from Table 1 that lattice parameter of $PNCa_3$ [20] is the smallest one due to the smallest atomic radius of P. There are no experimental data about bulk moduli and its pressure derivatives of these compounds in the literature for the comparison. Unlikely, the bulk moduli decrease with the increase in the atomic size of X atoms due to the relationship between bulk modulus and lattice constants which have an inverse proportion. It can be concluded from Tables 1 and 2 that the calculated value of Bulk modulus of elastic constants is close with one obtained from the EOS fitting. The calculated pressure derivatives of the bulk modulus (4.25 and 4.23 for Murnaghan and Birch Murnaghan EOS) for $PbNCa_3$ are well in agreement with theoretical values (4.2) [2]. The smallest one is obtained for $GeNCa_3$ [2], while the biggest one is for $SbNCa_3$ [14].

The normalized volume V/V_0 and lattice constants a/a_0 versus the pressure for $PbNCa_3$ are given in Fig. 2, where V_0 and a_0 are features of equilibrium structures at 0 GPa. It is shown in Fig.2 that the a/a_0 and V/V_0 ratios decrease as the applied pressure increases from 0 to 50 GPa. In order to define pressure dependence values under 0–50 GPa for the structural parameters, the curves in Fig. 2 are fitted to second-order polynomial:

$$a/ao = 0.99536–0.00428*P + 3.7205 \times 10–5*P2$$
$$V/Vo = 0.98461–0.01196*P + 1.13707 \times 10–4*P2$$

Electronic properties

The electronic properties of a material can be obtained by its band structure and density of states (DOS). The computed band structure along the high symmetry directions in the Brillouin zone can be seen in Fig. 3. The Fermi energy is set to zero. For this compound, the bands cross the Fermi level along the particular high symmetry lines of the first Brillouin zone. Energy gap near the Fermi level cannot be observed, and it shows the metallic properties for $PbNCa_3$, although the pressures increased up to 50 GPa.

The total and partial density of states is also given in Fig. 4a. It can be seen that the valence bands localized in two regions. Pb –5*d* states compose the lowest energy region of the valence band. Moreover, the hybridization of Pb –*6 s* and N –*2p* states compose the next bands below the Fermi level. Also, in the conduction band located above the Fermi energy level, Ca 3*p*-states and Pb-5*d*-states provide the major contribution.

The DOS of a system indicates the number of states at each energy level. The electronic behavior has been discussed through the DOS of $PbNCa_3$ in 0, 25, and 50 GPa given in Fig. 4b. It can be seen from Fig. 4b that the shapes of the curve under pressure have no a significant change, showing that the structure of $PbNCa_3$ is stable and no structural phase transformation occurs in the investigated pressures. By the comparison of the DOS in 0, 25, and 50 GPA, it can be seen in Fig. 4b

Table 2 Bulk modulus *B* (GPa), Young Modulus E (GPa), shear modulus *G* (GPa), Voigt shear modulus (Gv), Reuss shear modulus (G_R), G/B ratio, Poisson's ratio (υ), Zener Anisotropy factor (A), and elastic constants C_{ij} (GPa) of $PbNCa_3$ under zero pressure

P	B	E	G	G_V	G_R	G/B	υ	A	C_{12}	C_{11}	C_{44}
0 (This study)	50.77	77.81	31.26	33.39	29.13	0.615	0.24	2.14	37.57	77.18	42.45
Theory [2]	50	169	90					2.35	38	75	43
$GeNCa_3$ [2]	58	143	66					1.30	36	102	43
[23]	56.3	98.0	40.5					1.02	29.7	109.4	40.9
$SnNCa_3$ [2]	56	160	78					1.73	39	90	44

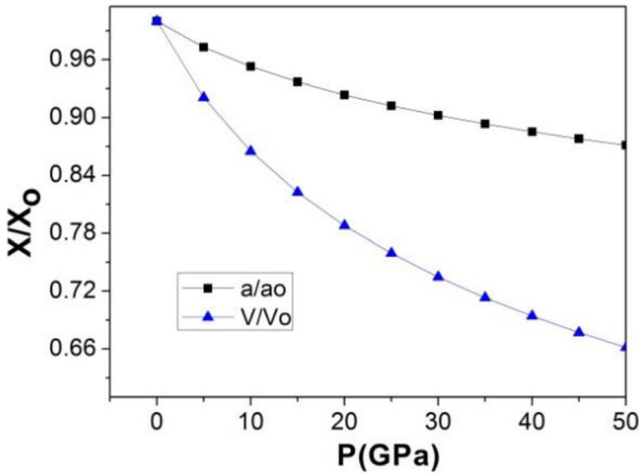

Fig. 2 Variations of lattice parameter and cell volume and of $PbNCa_3$ with pressure

that the TDOS below the Fermi level are pushed to lower energies, while the states above the Fermi level shift to the higher energies. These situations may be related to the smaller distance of atoms under pressure.

Elastic properties

Elastic constants are important parameters of material investigated which can provide a link between the mechanical and dynamical stability and give important information about the nature of the forces and bonding. We have calculated the elastic constants at calculated lattice parameters to study the stability of this compound using the stress-strain method.

In real materials, under high temperature, there are defects due to configuration entropy. The concentrations of the defects increase with increasing temperature. Thus, the experimental elastic constants are smaller than calculated values. The calculations of the elastic constants at zero temperature are useful due to check finite temperature elastic constants. And also because in some case, elastic constants are so small as to make calculations of finite temperature difficult. Finally, zero temperature elastic constants are much more economical than finite temperature elastic constants allowing a rapid exploration of the parameter, and they can be calculated much more accurately.

Besides these practical reasons, zero temperature elastic constants are also interesting due to the fact that these elastic constants show a new physical property of inhomogeneous system. Elastic constants can be defined by the derivative of the stress with respect to strain. When the system is strained, care should be taken to calculate the derivatives at zero force on each atom because there can be local rearrangements of the atoms.

Elastic constants tensor

$$C_{\alpha\beta\sigma\varepsilon} = -\frac{\partial t_{\alpha\beta}}{\partial e_{\sigma\varepsilon}}$$

At zero temperature

$$C_{\alpha\beta\sigma\varepsilon} = -\left.\frac{\partial t_{\alpha\beta}}{\partial e_{\sigma\varepsilon}}\right|_{F_{i=0}}$$

where the subscript indicates that the derivative must be performed at zero net force on each atom indicating the definition of the equilibrium at zero temperature [31].

Ternary $PbNCa_3$ compound is ideal cubic antiperovskite structure; therefore, C_{11}-, C_{12}-, and C_{44}-independent elastic constants are required to characterize elastic behavior. The second-order elastic constants (C_{ij}) at equilibrium lattice parameter have been computed to study the stability of this compound. The results of obtaining elastic constants are given in Table 2. From Table 2, it can be seen that the calculated elastic constants at $P = 0$ GPa and $T = 0$ K are in good agreement with those of Ref. [2] for $PbNCa_3$ and Ref. [2] and [23] for $GeNCa_3$ and $SnNCa_3$. Besides, the dependency of the elastic constants of pressure is a significant characterization of the crystals under varying pressure. The elastic constants as a function of pressure can be seen in Fig. 5. It is easy to observe in Fig. 5 that while C_{11}, C_{12}, and C_{44} elastic constants show

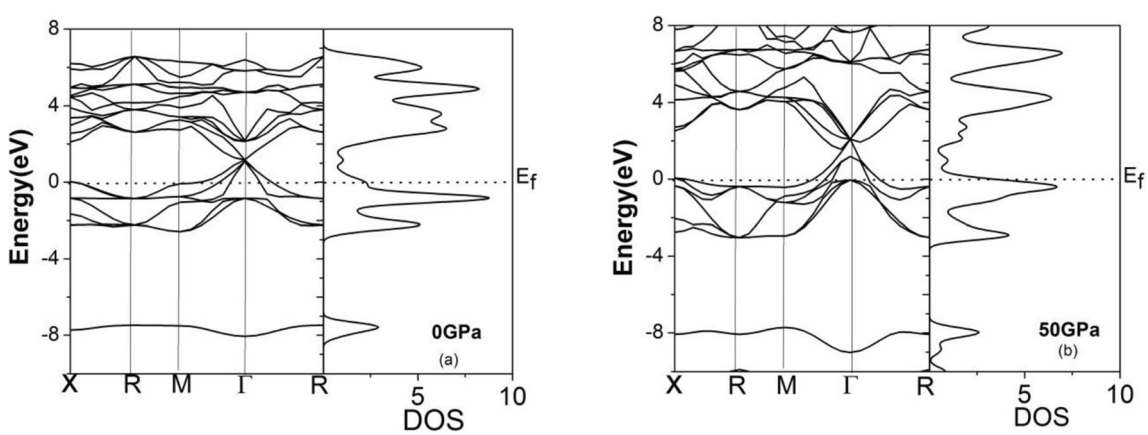

Fig. 3 Band structure and density of states for $PbNCa_3$ at (**a**) 0 GPa and (**b**) 50 GPa

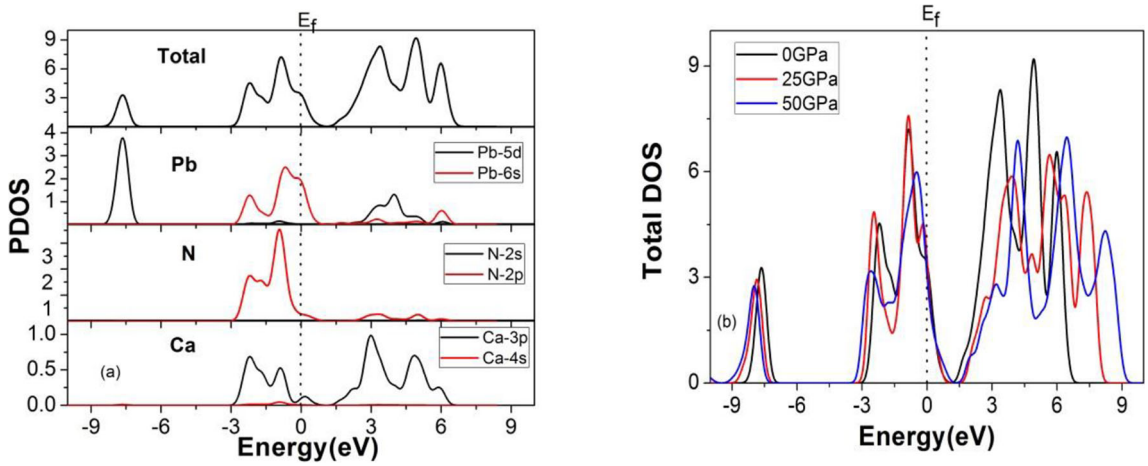

Fig. 4 Calculated (**a**) partial density of states and (**b**) total density of states under pressure for $PbNCa_3$

increment with the pressure. The C_{11} and C_{12}, which are due to the elasticity in length (the longitudinal distortion), rapidly increase with pressure. The C_{11} and C_{12} increase by 306.7% and 250.8% when the applied pressure change from 0 to 30 GPa. On the other hand, C_{44} increases by 63.3% with pressure. Indeed, the C_{44}, which is correlated with the elasticity in shape and gives a measure of stiffness against the shape deformation.

In order to be mechanically stable crystal, the second-order elastic constants must be positive. This definition is known as the Born stability criteria [32]: C_{11}-C_{12}>0, C_{11}>0, C_{44}>0, and C_{11}+2C_{12}>0, and these criteria are satisfied, indicating that this material is mechanical stability in this phase, implying all in the pressure range 0–30 GPa.

An elastic constant calculated correctly is very important in determining the mechanical features of the crystal. For a solid, Young's modulus (E), shear modulus (G), bulk modulus (B), etc., parameters contain the mechanical properties. The most important elastic parameters of materials such as anisotropy factor A, Young's modulus (E), shear modulus (G), bulk modulus (B), and Poisson's ratio are acquired from the calculated

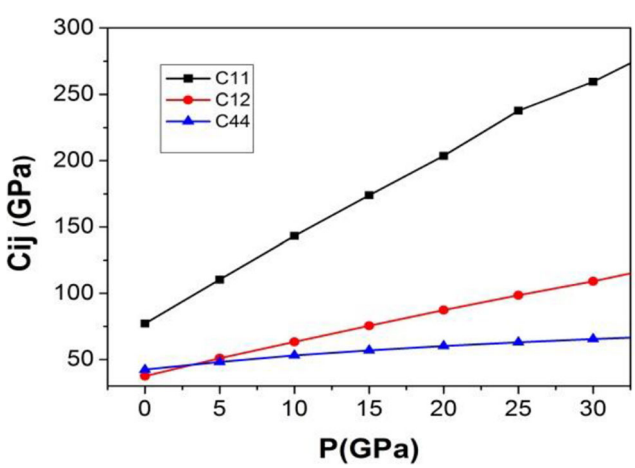

Fig. 5 Calculated pressure dependence of the elastic moduli at zero temperature

elastic constant C_{ij} utilizing the Voigt–Reuss–Hill (VRH) method [33]. For the cubic crystal, the Voigt [34] and Reuss and Angew [35] bounds of B and G are given as

$$B_v = B_R = B = \frac{C_{11} + 2C_{12}}{3} \tag{1}$$

$$G = \frac{1}{2}(G_v + G_R) \tag{2}$$

where G_V is Voigt's shear modulus corresponds to the upper bound of G values ($G_V = (C_{11} - C_{12} + 3C_{44})/5$) and G_R is Reuss's shear modulus corresponds to lower bound of G values ($5/G_R = 4/(C_{11} - C_{12}) + 3/C_{44}$). The elastic features such as the Young's modulus (E), Poisson's ratio (υ), and Zener anisotropy factor (A), which are the most interesting elastic features for utilizations are often analyzed for polycrystalline materials. These values are also calculated in terms of the computed using the following equations [36]:

$$A = \frac{2C_{44}}{C_{11} - C_{12}} \tag{3}$$

$$V = \frac{1}{2}\frac{B - \frac{2G}{3}}{B + \frac{G}{3}} \tag{4}$$

$$E = \frac{9GB}{G + 3B} \tag{5}$$

The calculated B from obtaining elastic constants, A, υ, E, G, G_V, G_R, and G/B ratio for $PbNCa_3$, can be seen in Table 2. The pressure dependence of B, G, and E are displayed in Fig.6a. The obtained B and G exhibit linear relationship with the applied hydrostatic pressure. E is defined as the ratio of the tensile stress to the tensile strain and is used to measure the stiffness of the materials. The larger the Young's modulus E, the stiffer the material is. The Young's modulus increases with

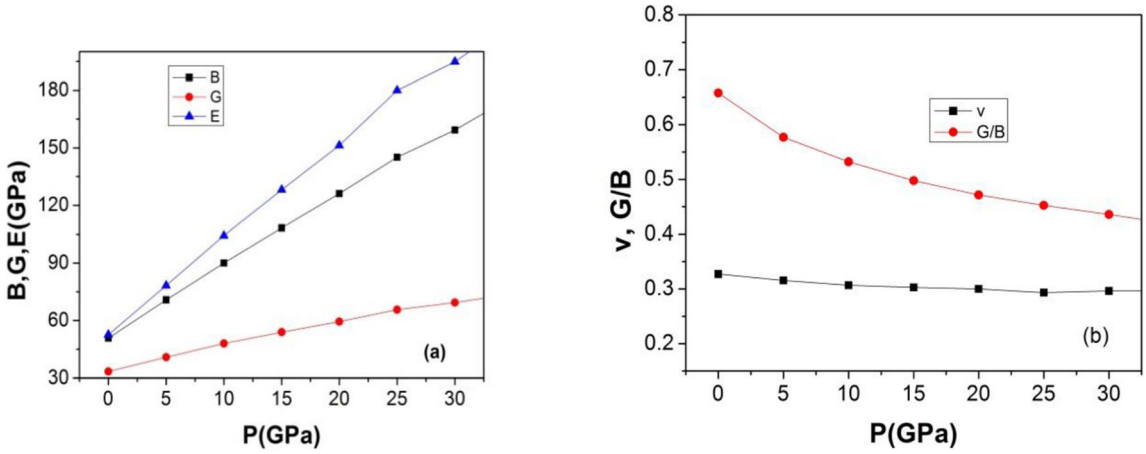

Fig. 6 (**a**) Bulk modulus *B*, shear modulus *G*, Young modulus E, and (b) B/G ratio and Poisson ratio υ of $PbNCa_3$ as a function of pressure at zero temperature

pressure indicating that the stiffness of $PbNCa_3$ compound can be increased by applying external pressure. For $GeNCa_3$ and $SnNCa_3$, the values of B, G, and E for $GeNCa_3$ and $SnNCa_3$ are higher than those of $PbNCa_3$ showing that these compounds are harder than that of $PbNCa_3$.

It can be seen in Table 2 that both Young's and shear modulus of $PbNCa_3$ are low, which designates it is a soft material.

The shear modulus (G) indicates the plastic deformation resistance, whereas the bulk modulus (B) indicates the fracture resistance. Pugh [37] formulated a simple relation between bulk and shear moduli (G/B) to estimate ductility. The critical value of the ratio G/B separating the brittle and ductile behavior of materials is around 0.57; i.e., if the G/B > 0.57, the material behaves in a brittle manner; otherwise, it behaves in a ductile manner. Here, the calculated value of the G/B ratio is greater than 0.57, indicating that this compound is brittle in nature as seen in Table 2. The values of G/B decrease in pressure (see Fig.6b). The value of lower limit and upper limit Poisson ratio (υ) are given as 0.25 and 0.5 for central forces in solids, respectively [38]. The values of υ are typically between 0.1 and 0.25 for covalent materials, and interatomic forces are non-central forces [39], while the lower and upper limits of υ are 0.25 and 0.5, respectively, and interatomic forces are central forces [40] for ionic crystals. In our case, υ value is equal to 0.327 at 0 GPa for $PbNCa_3$; i.e., the interatomic forces in the $PbNCa_3$ are central forces and have an ionic contribution in intra-atomic bonding. Now we also presented the pressure dependence of Poisson's ratio up to 30 GPa. We can see that Poisson's ratio increases linearly with pressure in Fig. 6b.

For an isotropic crystal, $C_{11}-C_{12} = 2C_{44}$, so A = 1, while any value smaller or larger than 1 indicates anisotropy. The *A* is a measure of the degree of elastic anisotropy in solids. The calculated *A* value for $PbNCa_3$ is equal to 2.14 at 0 GPa, which deviates in the positive direction from 1. This means that this material is an anisotropic compound and is lower than other theoretical result (2.35) [2].

The antiperovskite materials, including metals, semiconductors, insulators, and superconductors, are applicable in various technologies. In batteries, it is known that solids with superionic conductivity are better than organic liquid electrolytes [40]. Moreover, these materials have varied physical properties: giant magnetoresistance (GMR) [41], almost zero temperature coefficient of resistivity [42], and magnetostriction [43]. Antiperovskites are beneficial, especially in industrial impositions such as GMR. GMR is used in magnetic field sensors, used to read input in devices, also microelectromechanicals and biosensors. Besides, antiperovskites are proper material in all conditions because of its resistivity in zero temperature. Antiperovskites are also favorable in space and automobile technology because of its great mechanical characteristic [10, 44].

Vibrational properties

Phonons are the main stimulation that affects some physical properties, particularly the thermodynamic manner. For the investigation of vibrational features, we have investigated the phonon graph of $PbNCa_3$ compound.

The phonon dispersion relation and phonon density of states have been computed from the force constant method using density functional perturbation theory for $PbNCa_3$. For throughout this calculation, we used the CASTEP code with 2 × 2 × 2 supercell. The phonon dispersion spectrum along the high symmetry directions XRMΓR together with the total and partial phonon density is shown in Fig. 7 at 0 GPa and 50 GPa. In the cubic antiperoveskite-type $PbNCa_3$ primitive cell, there are five atoms. Due to this reason, there should be distribution of 12 optical and 3 acoustic. Moreover, in Fig. 7a, ternary $PbNCa_3$ shows no negative frequency which confirms that it is dynamically stable in this phase at 0 GPa. To see the dynamical stability of PbNCa3 under pressure, phonon frequencies of $PbNCa_3$ are calculated under 50 GPa. Under pressure, no imaginary frequency is found, implying that the

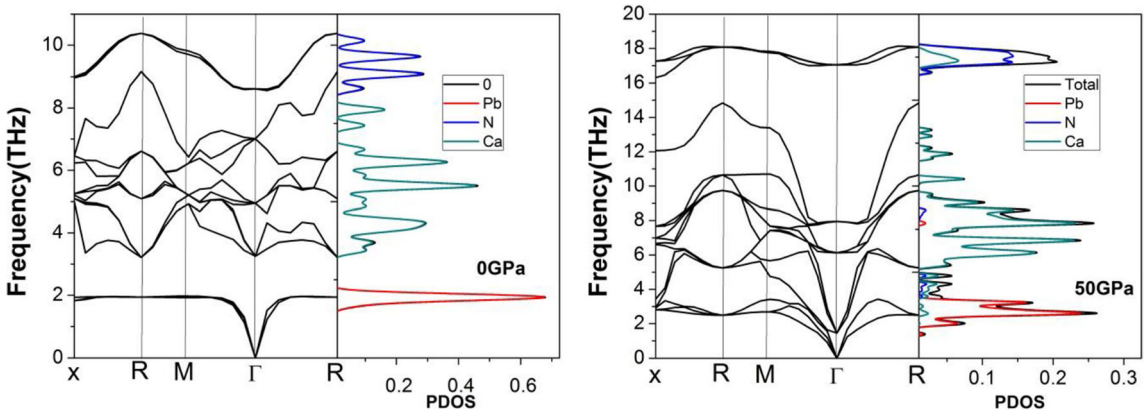

Fig. 7 Phonon dispersion curves (**a**) 0 GPa and (**b**) 50 GPa for $PbNCa_3$

Pm3m(221) structure of $PbNCa_3$ under pressure is dynamically stable. Unluckily, there is no available experimental data for $PbNCa_3$ compound based on phonon dispersion curves under pressure The magnitude of frequency increases with increasing pressure. From Fig. 7a, it can be seen that there is a gap in between 2 and 3.5 at 0 GPa, but under 50 GPa pressure, the gap disappears and the minimum point of optical branches at Γ point decreases with pressure, while the maximum point at the R point in optical phonon increases under pressure due to enhancement of interlayer interaction.

Because of the symmetry, the distinct number of phonon modes decreased along the high symmetry directions. The

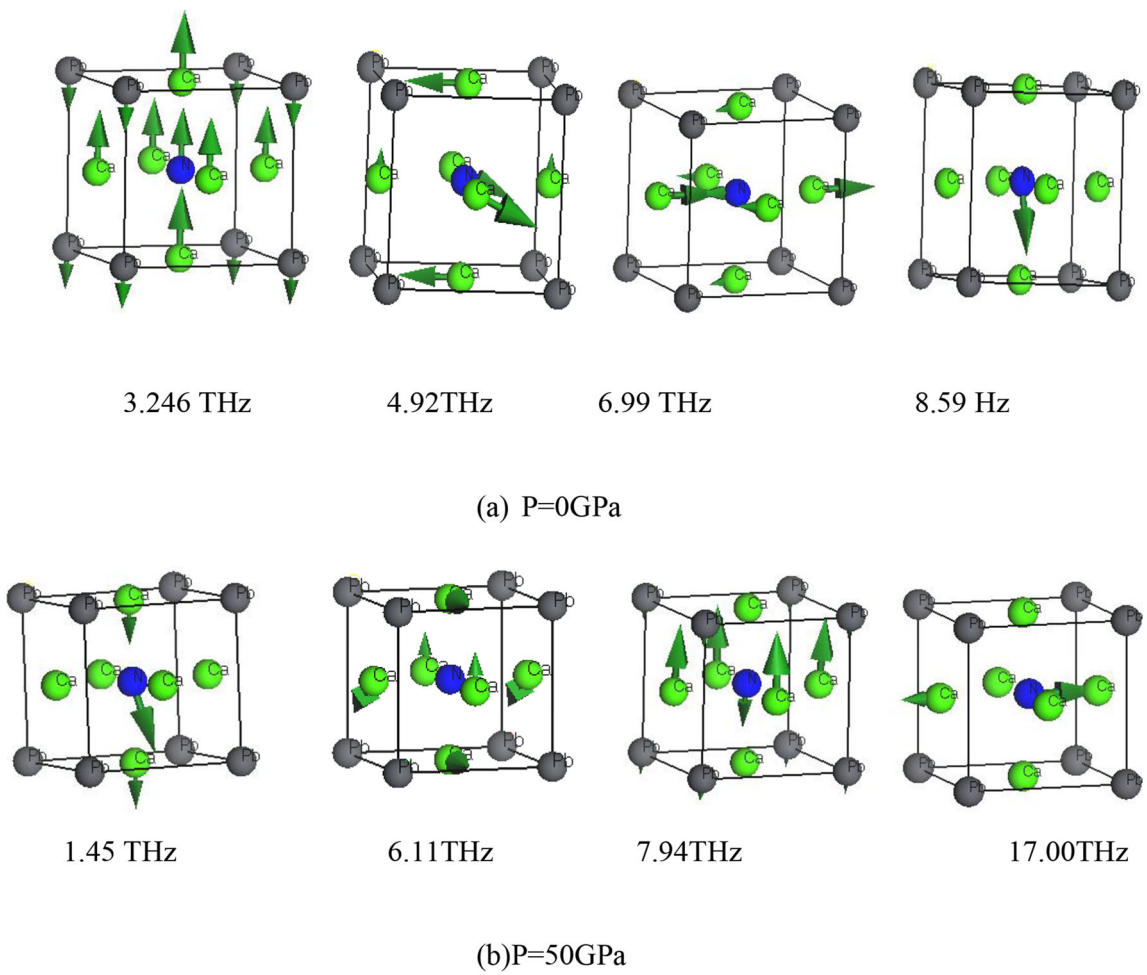

Fig. 8 Schematic eigen vector displacements of vectors representing the optical zone center Γ phonon modes at 0 GPa (**a**) and 50 GPa (**b**) for $PbNCa_3$

phonon dispersion curves indicate that the acoustic phonon frequencies are mostly due to Pb, since Pb atoms are heavier than N and Ca atoms which result in lower vibration. Mid frequency regions on the optical branches includes a vibration of Ca, while high frequency regions are due to N atoms for both pressures.

To understand the behavior of all phonon modes at Brillouin zone center, we have investigated the pressure dependency of the lattice vibrations at Γ point. According to group theory, the vibrations at Γ point in Pm3m structure of $PbNCa_3$ have the following irreducible representations:

$$\Gamma\ (\mathrm{Pm3m}) = 3\ \mathrm{T}_{1u} + \mathrm{T}_{2u}.$$

Three Tıu (triply degenerate) and T_{2u} irreducible representations are infrared (IR) active optical phonon modes. Calculated phonon modes in Thz unit are 3.25 (1.45), 6.99 (7.94), and 8.59 (17.00) Thz for T_{1u} and 4.94 (6.11) for T_{2u} at 0 (50) GPa. The pressure dependence of the phonon frequencies increases generally. Phonon vibration modes occurred by atomic vibrations. To investigate atomic displacement giving the vibration modes, the relevant phonon eigen vectors for T_{1u} and T_{2u} are shown in Fig. 8. The displacement figure associated with polar soft mode was induced by the displacement of Pb in one directions and the displacement of Ca and N ions in the opposite direction for 3.25 Thz at 0 GPa.

Conclusions

We have investigated that the computed electronic, mechanical, structural, and dynamic features of $PbNCa_3$ compound have been analyzed using DFT. Lattice parameter and cell volume are analyzed under pressure up to 50 gap, and it is found that it reduces with pressure. The computed elastic constants indicate that this compound exhibits mechanical stability in the cubic phase. $PbNCa_3$ compound has ionic bonding features, and its interatomic forces are central forces. In addition, we have computed the zone center vibrational frequencies of material with density functional perturbation theory approach. All the mode assignments were done and observed no negative phonon frequencies. This fact indicates that compound is dynamically stable in considering phase under pressure. The group theory analysis shows that there is no phase transition due to positive values of phonon mode in the interlayer for under pressure up to 50 GPa. The pressure dependency of the elastic features and their related values (B, G, and E) have been computed. The elastic constants and B, G and E quantities increase linearly from 0 to 30 GPa under pressure.

Funding This study was supported financially by the Research Center of Amasya University (Project No: FMB-BAP16-0202).

References

1. Souza ECCD, Muccillo R (2010) Properties and applications of perovskite proton conductors. Mater Res 13:385–394
2. Haddadi K, Bouhemadou A, Louail L, Medkour Y (2009) Structural, elastic and electronic properties of XNCa3 (X= Ge, Sn and Pb) compounds. Solid State Commun 149(15–16):619–624
3. Bilal M, Jalali-Asadabadi S, Ahmad R, Ahmad I (2015) Electronic properties of Antiperovskite materials from state-of-the-art density functional theory. J Chemother 2015:11
4. Kim WS, Chi EO, Kim JC, Choi HS, Hur NH (2001). Solid State Commun 119:507
5. Chi EO, Kim WS, Hur NH (2001). Solid State Commun 120:307
6. Bouhemadou A, Khenata R (2007). Comput Mater Sci 39:803
7. Okoye CMI (2006). Mater Sci Eng B 130:101
8. Ivanovskii AL (1995). Russ Chem Rev 64:499
9. Ivanovski AL, Sabiryanov RF, Skazkin AN (1998). Phys Solid State 40:1516
10. Tong P, Wang B-S, Sun Y-P (2013) Mn-based antiperovskite functional materials: review of research. Chin Phys B 22(6):067501
11. Takenaka K, Takagi H (2005) Giant negative thermal expansion in Ge-doped anti-perovskite manganese nitrides. Appl Phys Lett 87(26):261902–261902-3
12. Nakamura Y, Takenaka K, Kishimoto A, Takagi H (2009) Mechanical properties of metallic perovskite Mn3Cu0.5Ge0.5N: high-stiffness isotropic negative thermal expansion material. J Am Ceram Soc 92(12):2999–3003
13. Chern MY, Vennos DA, DiSalvo FJ (1992). Sol State Chem 96:415
14. Moakafi M, Khenata R, Bouhemadou A, Semari F, Reshak AH, Rabah M (2009). Comput Mater Sci 46:1051
15. Murnaghan FD (1944) The compressibility of media under extreme pressures. Proc Natl Acad Sci U S A 30(9):244–247
16. Niewa R, Schnelle W, Wagner F (2001) Synthesis, crystal structure, and physical properties of (Ca3N) Tl. Z Anorg Allg Chem 627(3): 365–370
17. Jäger J, Stahl D, Schmidt PC, Kniep R (1993) Ca3aun: Ein Calciumauridsubnitrid. Angew Chem 105(5):738–739
18. Papaconstantopoulos DA, Pickett WE (1992). Phys Rev B 45:4008
19. Vansant PR, Van Camp PE, Van Doren VE (1998). Phys Rev B 57: 7615
20. Haddadi K, Bouhemadou A, Louail L, Maabed S, Maouche D (2009). Phys Lett A 373:1777
21. Birch F (1978). J Geophys Res B 83:1257
22. Iqbal S, Murtaza G, Khenata R, Mahmood A, Yar A et al (201) Electronic and optical properties ofCa3Mn (M= Ge, Sn, Pb, P, as, Sb and Bi) antiperovskite compounds. J Electron Mater 45(8): 4188–4196
23. İyigör A, Al S (2019). Sakarya Univ J Sci 23(4):700–706
24. Bilal M, Ahmad I, Jalali Asadabadi S, Ahmad R, Maqbool M (2015). Electron Mater Lett 11(3):466–480
25. Segall MD, Lindan PJD, Probert MJ, Pickard CJ, Hasnip PJ, Clark SJ, Payne MC (2002). J Phys Condens Matter 14:2717
26. Hohenberg P, Kohn W (1964). Phys Rev B 136:864
27. Fischer TH, Almlof J (1992). J Phys Chem 96:9768
28. Perdew JP, Burke K, Ernzerhof M (1996). Phys Rev Lett 77:3865
29. Monkhorst HJ, Pack JD (1976). Phys Rev B 13:5188
30. Bilal M, Ahmad I, Aliabad HAR, Asadabadi SJ (2014). Comput Mater Sci 85:310
31. Lurtsko JF (1989). J Appl Hys 8:2991
32. Born M (1940) Math Proc Cambridge Philos Soc 36(2), 1 60
33. Hill R (1952). Proc Phys Soc A 65:349–354
34. Voigt W (1928) A determination of the elastic constants for beta-quartz Lehrbuch de Kristallphysik (Terubner, Leipzig)
35. Reuss A, Angew Z (1929). Z Angew Math Mech 9:49–58

36. Schreiber E, Anderson OL, Soga N (1973) McGraw- Hill, New York
37. Pugh SF (1954) London Edinburgh Dublin Philos. Mag J Sci 45: 823–843
38. Fu H, Li D, Peng F, Gao T, Cheng X (2008). Comput Mater Sci 44: 774
39. Haines J, Leger JM, Bocquillon G (2001). Annu Rev Mater Res 31: 1
40. Fu H, Li D, Peng F, Gao T, Cheng X (2003). Comput Mater Sci 774:23
41. Tangadurai V, Weppner W (2006) 81. Ionics 12:1
42. Kamishima K, Goto T, Nakagawa H et al (2001). Phys Rev B—Condens Matter Mater Phys 63(2):024426
43. Sun Y, Wang C, Chu L, Wen Y, Nie M, Liu F (2010). Scr Mater 62(9):686
44. Asano K, Koyama K, Takenaka K (2008). Appl Phys Lett 92(16): 161909

Publisher's note Springer Nature remains neutral with regard to jurisdictional claims in published maps and institutional affiliations.